Research Article

Vol. 28 (No. 4), pp. 296-307, 2025 doi: 10.5541/ijot.1684430 Published online: December 1, 2025

Comparative Study on The Effect of Oxygen-Enriched Air on Combustion of a Spark Ignition Engine Fuelled with Methanol and Ethanol

*1 Nidhi

¹ Department of Mechanical Engineering, Galgotias University, Greater Noida, Uttar Pradesh, India E-mail: *nidhi.tevatia@gmail.com

Received 26 April 2025, Revised 12 June 2025, Accepted 3 November 2025

Abstract

An experimental investigation was carried out on a single-cylinder four-stroke spark-ignition engine fuelled with methanol (M100) and ethanol (E100) to study the effect of oxygen enrichment on combustion characteristics of the engine. The experiments were carried out at base compression ratio 9.8 and the results were compared at higher compression ratio 10.6. The compression ratio was increased by decreasing the clearance volume from the cylinder head. The engine was operated at the maximum torque (4.5 Nm at 3600 rpm) achieved with M100 fuel and the results were compared for both the fuels at the same torque. The results indicate that with oxygen enrichment at the increased compression ratio, in-cylinder peak pressure increased significantly by 34.7% with M100 and 8.4% with E100 compared to base gasoline. The rate of pressure rise increased by 2.7 times with M100 and by 20% with E100. Due to high peak pressure, heat release rate, and rate of pressure rise, the combustion duration decreased significantly with both fuels. The cycle-to-cycle variation in indicated mean effective pressure decreased to 1.48% with E100 and M100. A notable outcome of the study was that the effect of oxygen enrichment was more prominent in methanol combustion than with ethanol at both compression ratios with greater effect at higher CR.

Keywords: Methanol; ethanol; combustion; IC engine; oxygen-enriched air.

1. Introduction

The utilisation of petroleum-based conventional fuels for transportation is a source of global problems including energy security, global warming, and poor local air quality. The transportation sector consumes 95% of the energy from gasoline and diesel [1]. Conventional fossil fuels are limited while the energy demand is rising rapidly. It is projected that coal reserves are available till 2112 and will be the only fossil fuel remaining after 2042. Oil and gas would have been diminished by that time [2]. The challenges of energy security and better climatic conditions have paved the path for the utilisation of alternative fuels such as ethanol and methanol in the transport sector. Ethanol and methanol are produced through well-established methods of biomass fermentation and coal gasification respectively. The physicochemical properties of the alcohol fuels including high flame velocity, high octane number, and low carbon to hydrogen ratio are suitable for their application in high compression ratio spark ignition (SI) engines. Most of the research work with ethanol and methanol fuels has been conducted with various blends of gasoline. The blending ratio of alcohol fuels with gasoline can be varied from 5% to 90% by volume. Various authors including, Tian et al. [3], and Pourkhesalian et al. [4] have reported that blends of alcohols (ethanol, methanol, and butanol) and gasoline improve the performance and decrease the emissions of carbonmonoxide (CO), hydrocarbon (HC), and oxides of nitrogen (NOx) from the engine.

High compression ratio and oxygen-enriched air for combustion are existing techniques to further enhance the performance of an alcohol-fuelled engine. The superior knock resistance of ethanol and methanol fuels allows for their application at a high compression ratio [5-9]. Awad et al. [10] reviewed the extensive literature on the impact of increasing compression ratio on performance, combustion, and emissions of the engine fuelled with oxygenated fuels such as alcohols and ethers. They reported that engine performance improved at high compression ratio (CR) and emissions of CO and carbondioxide (CO₂) decreased due to oxygen present in the fuels. High CR increased the flame speed and extended the air-fuel ratio and thus increasing the efficiency of the engine. Sakthivel et al. [11] reported that increasing the CR of the engine increased the peak pressure and heat release rate (HRR) in a motorcycle fuelled with E30 (ethanol gasoline blend). Balki and Sayin [12] reported that with the increase of CR, brake thermal efficiency (BTE) of the engine increased by 3.6% and 4.5% due to an increase in cylinder pressure which resulted in more work done by the piston. Prasad et al. [13] reported an increase in peak cylinder pressure with an increased compression ratio. Wouters et al. [14] reported that knock was not observed even at CR of 20.6 with methanol. In addition Gong et al., [15] Celik et al. [16], and Zhou et al. [17] reported the improvement of combustion, fuel economy, and emissions in engines fuelled with ethanol and methanol fuels at a high compression ratio.

The application of oxygen-enriched air to improve performance and control the emissions in an IC engine is a widely accepted method. Li et al. [18] reported that peak

*Corresponding Author Vol. 28 (No. 4) / 296

pressure and heat release increased with oxygen enrichment in an LPG fuelled SI engine. Emissions of CO and HC decreased and NOx increased due to high peak temperature and the presence of more oxygen during oxygen-enriched air. Caton [19] reported that increased cylinder pressure and temperature due to oxygen enrichment resulted in heat loss and decreased the thermal efficiency of the engine while emissions of NOx increased drastically. Seers et al. [20] reported that oxygen-enriched air resulted in fast flame propagation due to increased laminar flame speed and high initial mixture temperature during ignition timing in a SI engine. Nidhi and Subramanian [21] concluded a significant improvement in BTE of the engine and a reduction in CO and HC emissions from the engine. In addition, authors including Jeevahan et al. [22], Maxwell et al. [23], Quader [24], Kajitani et al. [25], and Poola et al. [26] reported that utilisation of oxygen-enriched air for combustion was beneficial to decrease the emissions from the engine.

The oxygen enrichment at increased compression ratio is a novel way to improve the combustion quality which would result in high thermal efficiency of the engine along with ultra-low emissions in ethanol and methanol fuelled SI engines. This experimental investigation was carried out at base and increased compression ratio to notice the effect of oxygen enrichment with two fuels ethanol and methanol. However, the literature survey indicates the studies on oxygen enrichment with conventional fuels such as gasoline and few studies are available with alcohol fuels. The literature survey does not indicate research work at increased compression ratio. This paper exclusively discusses the effect of oxygen enriched air on combustion characteristics of a SI engine including heat release rate, peak pressure, rate of pressure rise, combustion duration and coefficient of variance in IMEP in detail fuelled with two alcohol fuels.

2. Methodology

Maximum Brake Torque (MBT) timing for the study is the spark timing at which brake thermal efficiency of the engine is maximum. MBT timing for base gasoline, M100, and E100 fuels are determined experimentally. With M100, the maximum torque achieved was 4.5 Nm at 3600 rpm. The results obtained with methanol are compared with ethanol and BS-VI gasoline (base gasoline). The physicochemical properties of the fuels are given in Table 6. The engine characteristics are studied at the base condition with the fuels, then by oxygen enrichment (OE) at the base compression ratio of 9.8:1. Afterward, the compression ratio (CR) of the engine was increased to 10.6 and finally, oxygen enrichment was carried out at the increased compression ratio. For oxygen enrichment, the flow of oxygen was kept at maximum with both the fuels. The oxygen was injected into the intake manifold continuously (Figure 1). The enrichment level achieved was 30-40% (by mass) at the maximum torque condition. It was calculated as the percentage of oxygen supplied externally to oxygen present in the airflow. Since the maximum gas flow rate could not be changed due to which OE with M100 and E100 was not equal and lay in the range of 30-40%. With M100, it varied between 35-38% at both the compression ratios. The maximum oxygen flow rate is 0.22 g/s with the injector and it was obtained at 0.75 bar pressure beyond which the injector would close. The oxygen was injected into the intake manifold continuously. The maximum flow of oxygen from the injector was determined after several experimental trails. The working principle of the gas flowmeter is Coriolis with a maximum measurement error of \pm 0.5%. The gas is 99.9% pure in a high-pressure cylinder.

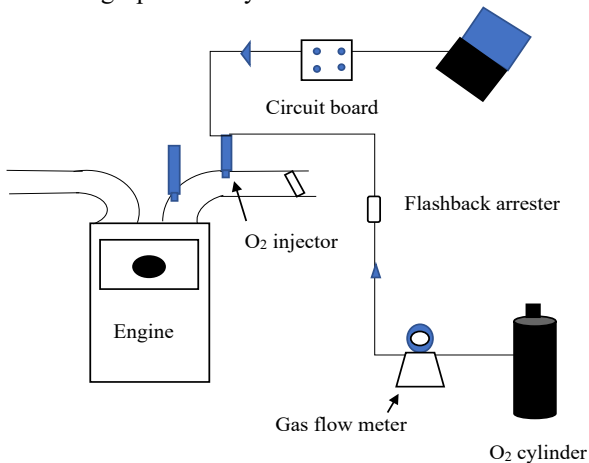


Figure 1. Oxygen enrichment method.

The compression ratio was increased by decreasing the clearance volume of the engine head [27] (Eq. (1)). It was performed by removing one layer from the gasket (fitted between head and liner) which was originally a pack of three layers as shown in Figure 2. Removing more than one layer could lead to the piston touching the head. Therefore, the removal of more than one layer was not carried out.

$$CR = 1 + \frac{V_{swept}}{V_{clearance}} \tag{1}$$

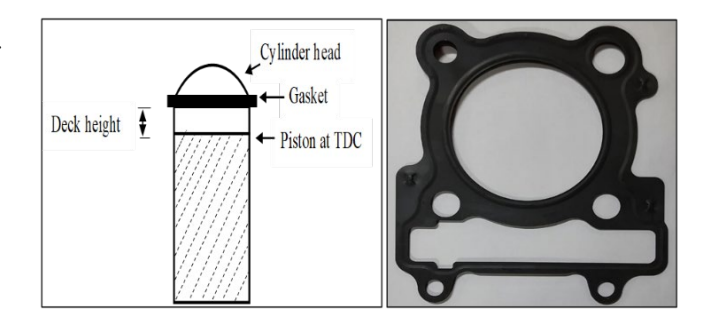


Figure 2. Schematic view of cylinder head with gasket and the original gasket.

Figure 2 shows the schematic view of cylinder head with gasket and the original gasket. Eqd. (2)-(5) were used for the calculation of the compression ratio. The original gasket of 1.3 mm thickness was replaced with thickness of 0.8mm (Figure 2). As a result, the volume of the gasket decreased which decreased the clearance volume of the engine head, thus compression ratio increased to 10.6:1. Swept volume (V_s) was calculated using Eq. (3). The calculated value is 249.32 cm³. *V_{crevice}* was measured by filling water inside the cylinder head. The calculated value is 19 cm³. The deck height is 0.8 mm given by the manufacturer which is used in Eq. (4) to calculate clearance gap height. The calculated gasket volume is 3.44 cm³ with thickness 0.8 mm. The increased compression ratio is 10.6:1.

$$V_C = V_{gasket} + V_{clearance gap} + V_{crevice}$$
 (2)

Swept volume
$$V_s = \frac{\pi}{4}B^2 \times L \tag{3}$$

$$\frac{\pi}{4}B^2 \times deck \ height \tag{4}$$

Volume of metal gasket

 $\frac{\pi}{4}B^2 \times \text{clearance gasket thickness} \tag{5}$

2.1 Experimental Details

The experiments were conducted on a single-cylinder four-stroke spark ignition engine having port injection. Valve timing diagram of the engine is given in Figure 3. The details of the engine are given in Table 1. The schematic layout of the experimental setup is given in Figure 4. An eddy current water-cooled dynamometer was used for applying load on the engine. The data was acquired at the maximum torque (4.5 Nm at 3600 rpm) achieved with methanol (M100) and compared with E100 at the base compression ratio. The throttle was fully opened at maximum torque point with methanol. The intake pressure for the condition was 1 bar. The volumetric efficiency of the engine was 83%. The MBT with M100 and E100 was 45 bTDC while with base gasoline it was 42 bTDC. MBT timings were found after several repeated experiments. Although methanol and ethanol have higher flame velocities than gasoline, their strong charge-cooling effect due to higher latent heat of vaporization and larger fuel mass requirement necessitates slightly earlier ignition to achieve the optimal cylinder pressure phasing.

Table 1. Engine specifications.

Table 1. Engine specifications.		
Engine	Single cylinder, four- stroke air-cooled	
Cylinder bore	74 mm	
Stroke	58 mm	
Compression ratio	9.8:1	
Swept Volume	250 сс	
Length of connecting rod	112 mm	
Lubrication	Forced	
Fuel injection	Port type	
Max. power output @ 8000 rpm	20 to 25 H.P	
Max. torque output @ 6000 rpm	18 to 20 Nm	

The equivalence ratio was stoichiometric for the fuels. It was controlled through a lambda sensor fitted to the exhaust side of the engine. An open ECU was used for controlling spark timing and equivalence ratio. A flashback arrester was used to control backfire propagation during oxygen enrichment. The uncertainty, sensitivity and other specifications of the instruments including air flow meter, fuel flow meter, dynamometer, crank angle encoder, pressure sensor and combustion analyser are given in Table 2 to 5. The fuel flow rate and oxygen gas flow rate were measured with a Coriolis principle-based flowmeters. Thermal based air flowmeter was used for measuring the air flow rate. The engine was run for 20-25 minutes to get it stabilized before storing the data. The data for in-cylinder pressure and corresponding crank angle was acquired using a piezoelectric-based pressure sensor fitted in the engine head and an optical-based crank angle encoder fitted on the dynamometer side. The pressure theta data was acquired

using AVL Indicom software, version 2.1. To study cycle to cycle variations in pressure, 500 cycles were acquired for analysis.

Table 2. Specifications of air flow meter.

S. No.	Parameter	Values/description
1	Make	Endress+Hauser (EH)
2	Measuring principle	Thermal mass flow
3	Operating temperature range	0-500C
4	Accuracy	+-1.5%

Table 3. Specifications of fuel flow meter.

S. No.	Parameter	Values/description
1	Make and Model	Rheonik, RHM015L
2	Working Principle	Coriolis
3	Temperature range	-20 to 1200C
4	Mass flow uncertainty	< 0.10%

Table 4. Specifications of dynamometer.

S. No.	Parameter	Values/description
1	Make and Model	Technomech, TME -50 (7.5 kW)
2	Туре	Eddy Current Water- Cooled Dynamometer
3	Maximum Power	37 kW
4	Maximum Torque	100 Nm
5	Cooling Media	Water
6	Direction of rotation	Bi – directional

Table 5. Specifications of crank angle encoder, pressure sensor and combustion analyser.

S. No.	Parameter	Values/description
1	Combustion Analyser Make and Model	AVL, IndiMicro 602TM
2	Linearity	±0.01% FS
3	Input Range (Piezo)	Up to 14,400 pC
4	Angle Encoder Make and Model	AVL, Angle encoder 366C
5	Engine speed measuring range	0-20,000 rpm
6	Resolution	0.5 CA.
7	Crank angle Signal	720 crank angles
8	Pressure Sensor Make and Model	AVL, GH15D
9	Working Principle	Piezoelectric Pressure Sensor
10	Sensitivity	19 pC/bar
11	Measuring Range	0-250 bar

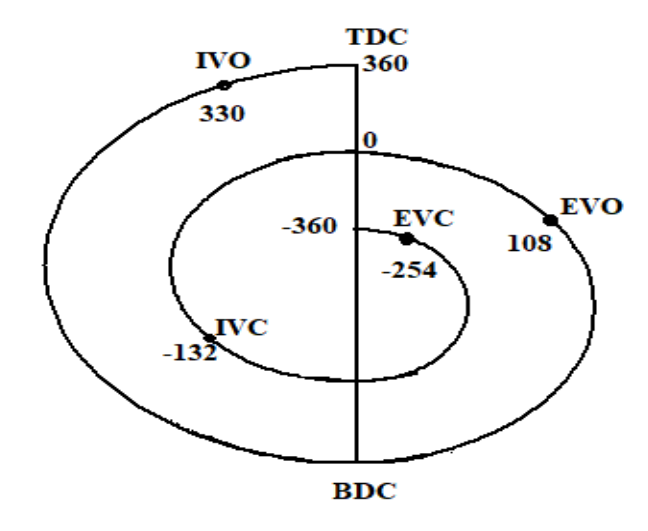


Figure 3. Valve timings of the engine.

Table 6. Physicochemical properties of ethanol, methanol and gasoline [12, 28, 29].

Properties	Gasoline	Methanol	Ethanol
Composition	>C ₈	СН ₃ ОН	C ₂ H ₅ OH
Carbon (% mass)	86	37.48	52.14
Hydrogen (%mass)	14	12.58	13.13
Oxygen (% mass)	0	50	34.7
Density STP, kg/m3	740	790	790
Dynamic viscosity (200C, mPa)	0.6	0.57	1.2
RON Research octane number (min.)	95	109	109
MON Motor octane number (min.)	85	92	98
Flash point (0C)	-45	11	14
Auto ignition temperature (0C)	465-743	738	698
Boiling point (0C)	25-215	65	79
Latent heat of vaporisation (kJ/kg)	180-350	1100	838
Low calorific value (MJ/kg)	43	20	26.95
Adiabatic flame temperature (K)	2275	2143	2193
Minimum ignition energy in air (mJ)	0.25	0.14	0.23
Quenching distance (mm)	2	1.85	1.65
Flame speed (cm/s)	28	52	39
Stoichiometric air/fuel ratio	14.5	6.5	9

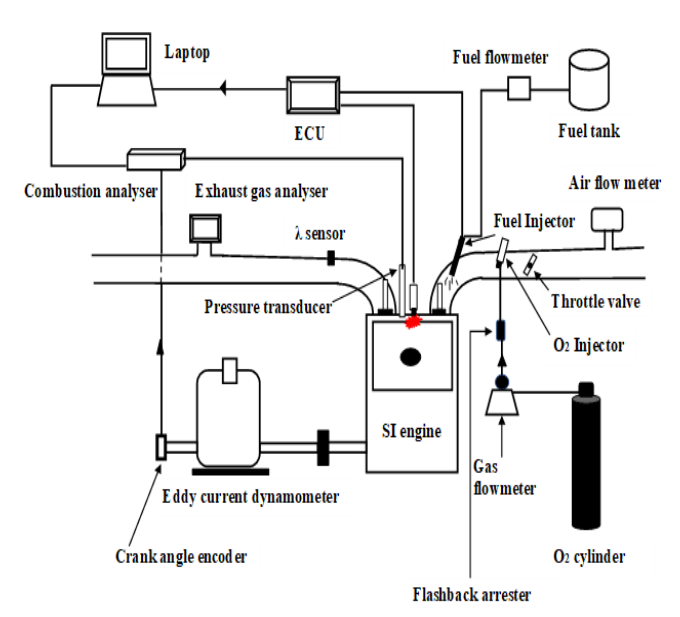


Figure 4. Experimental setup.

2.2 Mathematical Relations Used for Calculation

The net heat release rate (Q) was calculated using the first law of thermodynamics as given in Eq. (6) [27].

$$\frac{dQ}{d\theta} = \frac{\gamma}{\gamma - 1} P \frac{dV}{d\theta} + \frac{1}{\gamma - 1} V \frac{dP}{d\theta}$$
 (6)

where P, V, γ , and θ represent the in-cylinder pressure (pascal), instantaneous cylinder volume (m³), the ratio of specific heats, and the crank angle, respectively. The rate of pressure rise is calculated using Eq. (7). The ignition delay (ID) was calculated by using Eq. (8). The combustion duration (CD) was calculated by using Eq. (9).

$$\frac{dP}{d\theta} = P_i - P_{i-1} \tag{7}$$

where P_i is the pressure at a crank angle

$$ID = \int_{Spark}^{SOC} d\theta$$
 (8)

$$CD = \int_{SOC}^{EOC} d\theta \tag{9}$$

where, SOC- Start of combustion (crank angle (C.A) at which 10% of the maximum cumulative heat is released), EOC- End of combustion (C.A at which 90% of the maximum cumulative heat is released), ID- Crank angle duration of ignition timing and SOC, CD- Crank angle duration between SOC and EOC.

Net indicated mean effective pressure (IMEP $_{net}$) is calculated by Eq. (10).

IMEPnet =
$$\int_{-360}^{+360} PdV$$
 (10)

Coefficient of variance (COV) in $IMEP_{net}$ was calculated by Eq. (11).

$$COV_{IMEPnet} = \frac{\sigma_{IMEP_{net}}}{\mu_{IMEP_{net}}} \times 100\% \tag{11}$$

3. Results and Discussion

3.1 Variation of Peak Pressure and Its Crank Angle Position

With oxygen enrichment, peak pressure (P_{max}) increased by 56.5% with M100 and by 17.6% with E100 compared to base gasoline (Figure 5). The position of P_{max} shifted to 6 deg aTDC and 18 deg aTDC with M100 and E100 which was 23 aTDC with base gasoline. The distinct separation of the methanol curve in the in-cylinder pressure graph is primarily attributed to methanol's significantly higher laminar flame speed compared to both gasoline and ethanol. This characteristic leads to faster combustion and a more rapid pressure rise within the cylinder. Consequently, the spark timing for methanol was advanced closer to TDC to optimize peak pressure timing, resulting in a noticeably different pressure trace.

Various comparative studies confirm that P_{max} is higher with M100 than E100 [30-32]. The generation of OH radicals is more with M100 than E100 and gasoline. M100 does not contain carbon to carbon bond as found in E100. Inherently, the flame speed of M100 is greater than E100 and gasoline which is further enhanced due to oxygen enrichment [33]. The effect of oxygen enrichment was thus, more prominent with M100 than with E100. The combustion efficiency with methanol is higher than ethanol since number of intermediate products formed during its combustion are less than ethanol which adds to lower irreversibility and improved combustion [34].

Due to oxygen enrichment (OE) of intake air, the amount of nitrogen decreased which has higher specific heat (1.03 kJ/kg-K at 300 K, 1.21 kJ/kg-K at 1300 K) than oxygen (0.9 kJ/kg-K and 1.12 kJ/kg-K at 1300 K). When the nitrogen percentage decreases, the in-cylinder temperature increases. The high in-cylinder temperature promotes a faster rate of the chemical reaction. The oxygen helps in the generation of OH radicals which promotes the chain propagation of chemical reactions.

At a high compression ratio, P_{max} increased by 8% with both M100 and E100 compared to their values at base CR as shown Figure 6. The position of P_{max} shifted closer to TDC compared to the base compression ratio. The gain in peak pressure and shift in crank angle position can be attributed to the thermodynamic effects of higher compression ratios, which inherently raise the temperature and pressure of the intake charge during the compression stroke. These elevated thermodynamic conditions significantly enhance the flame propagation speed. The laminar flame speed is known to be a function of the initial pressure, temperature, and density of the unburned air-fuel mixture; thus, increased pressure and temperature at higher CR directly contribute to faster combustion kinetics [11].

For alcohol-based fuels such as M100 and E100, which already exhibit high flame speeds due to their oxygenated molecular structures and lower hydrocarbon chain lengths, the increase in CR further amplifies this behavior. Consequently, the combustion process becomes more rapid and complete, resulting in a steeper pressure rise and a higher peak pressure. This also causes the peak pressure to occur earlier in the cycle (closer to TDC), improving thermal

efficiency but potentially increasing the mechanical and thermal loads on engine components.

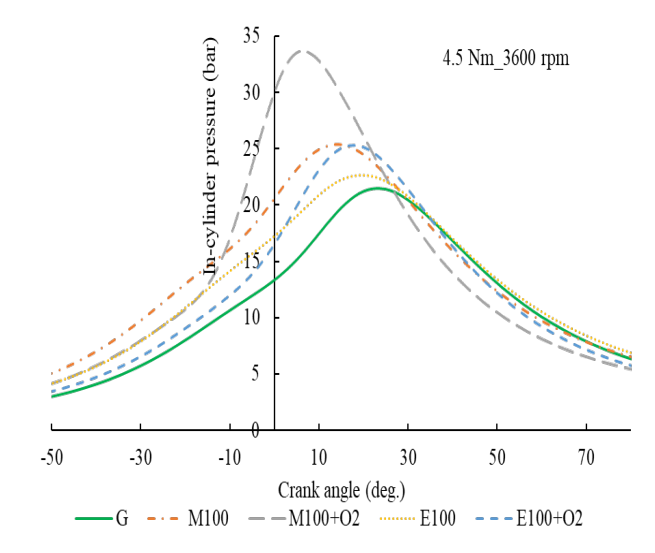


Figure 5. In-cylinder pressure variation with crank angle at base compression ratio with both fuels.

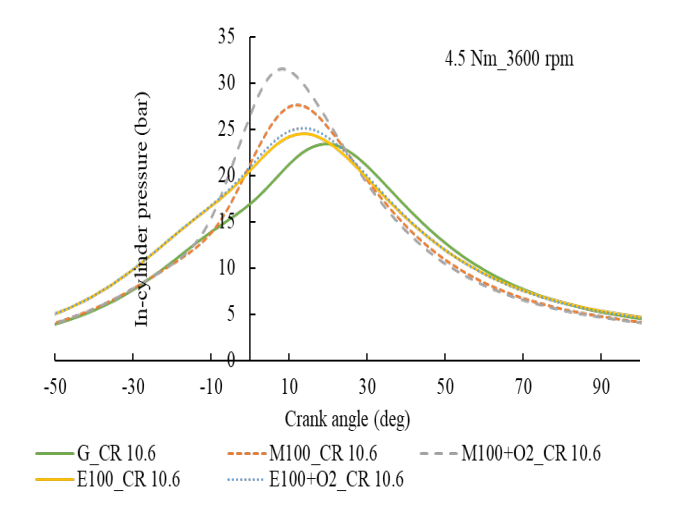


Figure 6. In-cylinder pressure with M100 and E100 at 4.5 Nm, 3600 rpm at 10.6 CR.

With oxygen enrichment at high CR (Figure 7), P_{max} increased by 34.7% and 8.4% with M100 and E100 compared to base gasoline. The position of P_{max} was 8 aTDC with M100 and 14 aTDC with E100. Eqs. (12) and (13) [21] show that with an increasing amount of oxygen, the rate of chemical reaction could be enhanced during the combustion of fuel. This is the famous Arrhenius Equation which indicates the temperature dependency of reaction rates.

Fuel + oxygen/air
$$\rightarrow$$
 products (12)

$$R_{r} = Ae^{\frac{-E_{a}}{RT}}[Fuel]^{a}[Oxygen]^{b}$$
 (13)

where A is the Arrhenius constant, Ea is the activation energy, R is the universal gas constant and T is the absolute temperature of the reaction.

With the added benefit of high CR, high temperature and pressure of reactants improve the growth of flame kernel and increase the flame propagation speed [35]. These factors result in better combustion with oxygen enrichment at high CR. At elevated CRs, the end-of-compression temperature and pressure rise significantly due to increased isentropic

compression work. This enhances the pre-flame reactions, facilitates autoignition, and supports the rapid growth of the flame kernel. A higher initial pressure also increases the density of the mixture, which according to laminar flame speed theory, increases the flame propagation speed due to the enhanced molecular collision frequency and reduced mean free path. Furthermore, oxygen enrichment increases the local oxygen availability in the flame front, leading to intensified exothermic reactions and a steeper pressure rise during the premixed combustion phase.

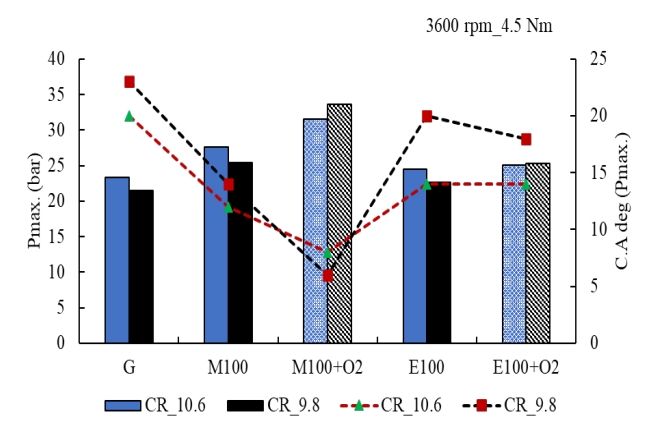


Figure 7. Comparison of P_{max} and corresponding crank angle with M100 and E100 at 4.5 Nm, 3600 rpm at different conditions.

3.2 Variation of Heat Release Rate (HRR), Combustion Duration, and Ignition Delay

With oxygen enrichment, max. HRR increased by more than 92.2% with M100 and by 65.4% with E100 compared to base gasoline. Combustion duration (CD) shortened by 35.8% with M100 and 28.2% with E100 compared to base gasoline. Furthermore, ignition delay (ID) shortened by 32% with M100 and was comparable to base gasoline in E100 (Figure 9).

M100 and E100 are neat (homogeneous) substances with a single boiling point. Gasoline does not behave like alcohol as it consists of different hydrocarbons. It has higher T90 (90% evaporation corresponding to the temperature) than alcohol fuels. Therefore, some fraction needs a high temperature for combustion. With oxygen enrichment, the flame speed and burning rate of charge are more pronounced since in-cylinder pressure and temperature are higher. It enhanced the HRR even better with M100 and E100 taking the added advantage of their lower boiling points. Figure 10 shows the cumulative heat release with both fuels at increased CR.

With a high heat release rate, the burning speed of charge is enhanced which shortened the CD with alcohol fuels. ID depends on the latent heat of vaporisation. When cylinder temperature is higher due to oxygen enrichment, alcohol fuels might evaporate quickly, thus shortening the ignition delay period. Overall, the effect of oxygen enrichment was more significant with M100 than with E100 as discussed previously.

At high compression ratio, max. HRR increased by 3% with M100 compared to base CR and was similar to base CR with E100. CD shortened by 20% with M100 and 2.7% with E100 compared to their respective values at base CR. ID decreased by 11.1% with M100 and by 9.8% with E100 compared to base CR. The CD and ID shortened by 8% and 12.2% at high CR compared to base CR.

At high CR, residual gases are lower and turbulence is more. As a result, rapid charge burning resulted in a shortened combustion duration and ignition delay with M100 and E100 compared to the values at the base compression ratio. The effect of increased CR is more significant with M100 and E100 than with gasoline for obvious reasons of their physico-chemical properties.

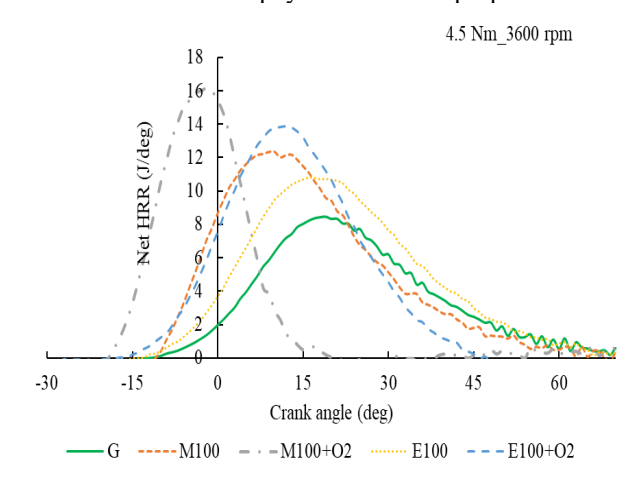


Figure 8. Net heat release rate with M100 and E100 at 4.5 Nm, 3600 rpm at both CRs.

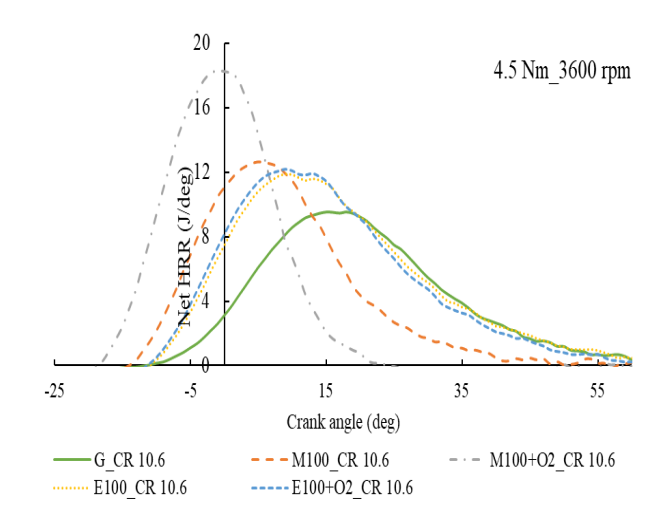


Figure 9. Net heat release rate with both fuels at 10.6 CR.

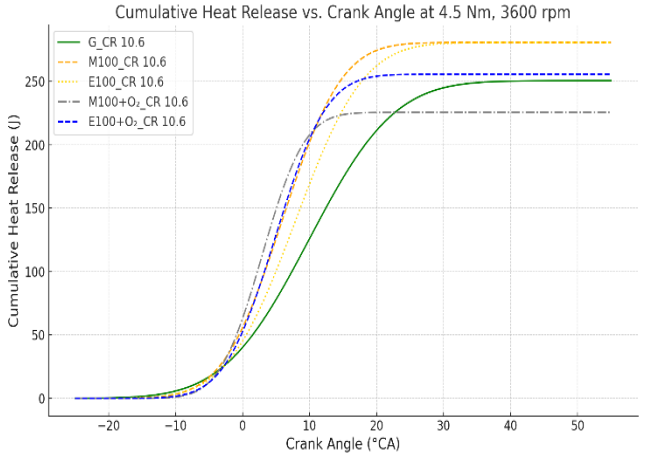


Figure 10. Cumulative heat release with both fuels at 10.6 CR.

With oxygen enrichment at high CR, max. HRR doubled with M100 and increased by 35.4% with E100 compared to base gasoline at high CR as shown in Figure 9. ID decreased by 32% with M100 compared to base gasoline at high CR

and by 10% with E100. CD shortened by 45.9% with M100 and by 8.1% with E100 compared to base gasoline at higher CR. The cumulative heat release (CHR) curves at 4.5 Nm and 3600 rpm shown in Figure 9 depicts that methanol (M100) and ethanol (E100) exhibit faster and earlier combustion compared to gasoline, due to their higher laminar flame speeds and oxygen content. Among all, methanol with oxygen enrichment (M100+O2) shows the steepest and earliest rise in CHR, indicating highly reactive and concentrated combustion. Ethanol with oxygen (E100+O₂) also shows enhanced combustion, though slightly less aggressive than methanol. In contrast, gasoline shows a delayed and broader CHR profile due to slower combustion kinetics. The leftward shift of CHR curves with oxygen enrichment confirms improved combustion phasing, which can enhance thermal efficiency if appropriately controlled.

Oxygen enrichment and high compression ratio both improve the combustion by enhancing flame propagation which contributes to shorter combustion duration [36]. Due to the rapid rate of reaction, the ignition delay period shortened with M100 and E100. With the high cylinder temperature, the vaporisation of E100 and M100 might also improve which could help to shorten ignition delay. Maximum HRR values for M100 are better than E100 because of the better combustion rate (Figure 11). It is well indicated through its high P_{max} and high max. ROPR values. Similar study from the literature reports that with oxyfuel combustion, at higher compression ratio the ignition delay shorten significantly with the improvement of cylinder pressure and fuel economy in a dual fuel spark ignition engine [37]. After most of the combustion is complete for fast-burning fuels (especially with oxygen enrichment), the remaining HRR signal is small in magnitude and more susceptible to signal noise. This is the reason of waveform pattern visible at the end of HRR curve. In addition to this, SI engines, especially under low load, exhibit cycle-to-cycle variation due to turbulence and fuel-air mixing dynamics. This is discussed in the subsequent section.

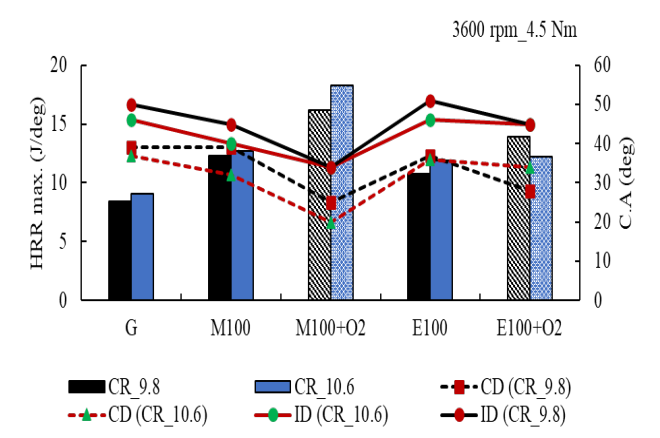


Figure 11. Comparison of max. HRR, combustion duration, and ignition delay with M100 and E100 at different conditions at 4.5 Nm, 3600 rpm.

3.3 Variation of Maximum (Rate of Pressure Rise) ROPR And Its Crank Angle Position

OE increased the max. ROPR by more than 2.5 times with M100 and 40.8% with E100 compared to base gasoline (Figure 12). The positions shifted much closer to TDC. With M100 and E100, it was 4 deg bTDC and 4 deg aTDC.

Max. ROPR was higher with M100 than with either base gasoline and E100. ROPR depends on various factors such as flame speed, turbulence inside the cylinder, the calorific value of the fuel, latent heat of vaporisation, and oxygen content [38-40]. High calorific value and turbulence result in high ROPR. The calorific values of M100 and E100 are lower than gasoline. Their flame speed and oxygen content ensure better and complete combustion which results in a high rate of pressure rise. Furthermore, methanol is a highly reactive fuel. All these factors increased the rate of pressure rise with M100. These factors would dominate the effect of its lower calorific value which could have decreased the ROPR. In the case of E100, the flame speed is not as high as M100 causing low ROPR. In addition to this, E100 breaks into triatomic molecules having high specific heat which lowers the in-cylinder temperature, and thus the rate of pressure rise could decrease. Since OE results in enhanced flame speed and combustion rate, ROPR would increase. More oxygen helps in the proper mixing of air and fuel and improves the combustion hence rate of pressure rise could increase.

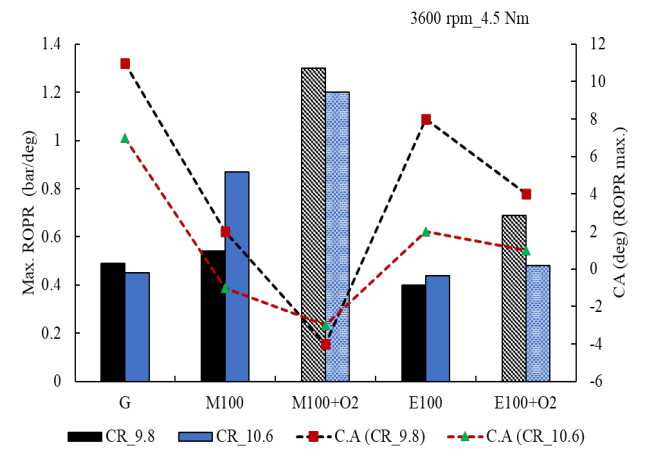


Figure 12. Comparison of max. ROPR with M100 and E100 at different conditions.

At high compression ratio, max. ROPR increased by 61% to 0.87 bar/deg with M100. With E100, it increased by 10%. At high CR, the positions were -1(bTDC) and 2 deg (aTDC) with M100 and E100. A high compression ratio increases the temperature as well as turbulence in the cylinder. As a result, the rate of heat release is improved which increased the maximum rate of pressure rise with alcohol fuels. Compared to gasoline, max. ROPR with E100 was slightly less at high CR. The low calorific value might lead to the generation of a low rate of pressure. It is clear from the values of peak pressure with E100 also, which is higher than gasoline but not at the level of M100. In this context, the fact that the reactivity of methanol is higher than E100, cannot be ignored.

With OE at high CR, max. ROPR with M100 increased by 2.7 times and with E100 by 20% compared to base gasoline. The corresponding crank angle positions advanced by 5 and 7 deg with M100 and E100. The positions were -3 (bTDC) and 1 deg (aTDC) with OE at high CR which was 7 deg (aTDC) with base gasoline. The degree of constant volume combustion is thus enhanced with OE at high CR.

In this method, the individual effect of OE and increased compression ratio is combined and in combination, the effect is more pronounced. With OE, the generation of active radicals such as OH, O, H etc. is more which caused rapid heat release, and thus the rate of pressure rise increases. In

addition, the turbulence level increases, and residual gas fraction decreases at high CR. All these factors contribute to high in-cylinder temperature and high rate of pressure rise.

3.4 Cycle-To-Cycle Variations in Imepnet

Figure 13 and 14 show the COV in IMEP with M100 and E100 fuels. The COV_{IMEP net} decreased from 2.38% to 1.97% with M100 and from 3.8% to 2.98% with E100 with oxygen enrichment (Figure 15). It should be noted that the experiments were conducted using an older dynamometer setup, which may have contributed to higher apparent frictional losses and deviations between IMEP and brake mean effective pressure values (BMEP). However, this does not affect the reliability of the comparative results and the observed trends between ethanol, methanol, and gasoline. Oxygen enrichment reduces the cyclic fluctuations in initial flame formation [35]. It implies that flame development and flame propagation are improved with oxygen enrichment resulting in better combustion. Therefore, cycle-to-cycle variations decreased with M100 and E100.

A lean mixture, incomplete combustion, low flame speed, and less ignition intensity are some of the factors which contribute to the cycle-to-cycle variations during combustion in SI engines [41]. The burning rate of charge inside the cylinder is influenced by variations in gas motion, amount of air, fuel, recycled exhaust gas, residual gases, and mixture composition near the spark plug. These factors depend on engine design and operating parameters and affect the cyclic variations [42].

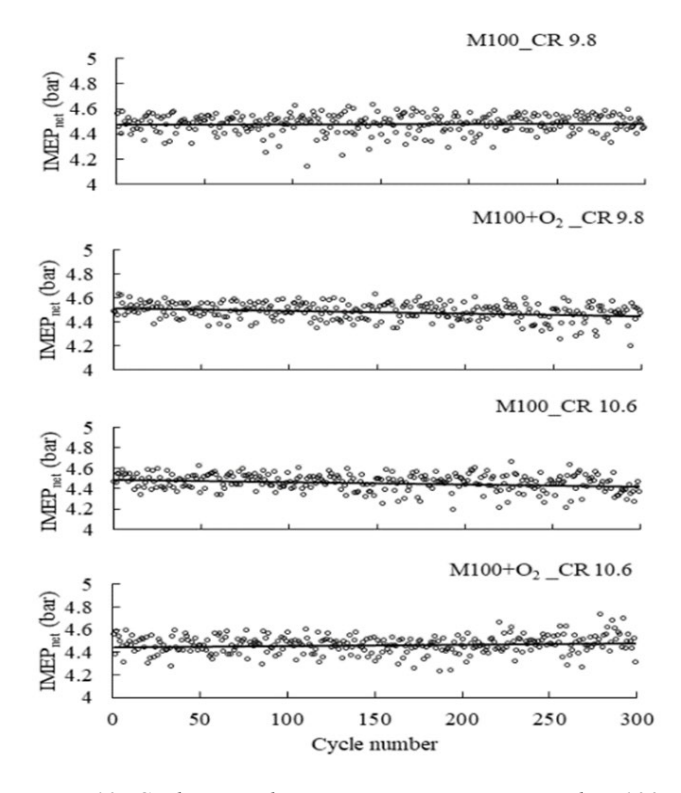


Figure 13. Cycle-to-cycle variations in IMEPnet with M100 at various conditions.

With the increase of compression ratio, the turbulence intensity increases, and cylinder pressure and temperature both increases. Squish intensity increase and combustion duration decrease at high CR. It improves flame kernel growth and thus flame propagation. As a result of this, the COV_{IMEP} decreased with M100 and E100 to 1.67%. With the increase in compression ratio, the cycle-to-cycle variations

decrease due to engine operation at high temperatures. The amount of residual gases decreases at high CR. The amount of residual gases change in every cycle. The decrease in their fraction and increase of turbulence and flame speed at high CR results in the decrease of the cycle-to-cycle variations.

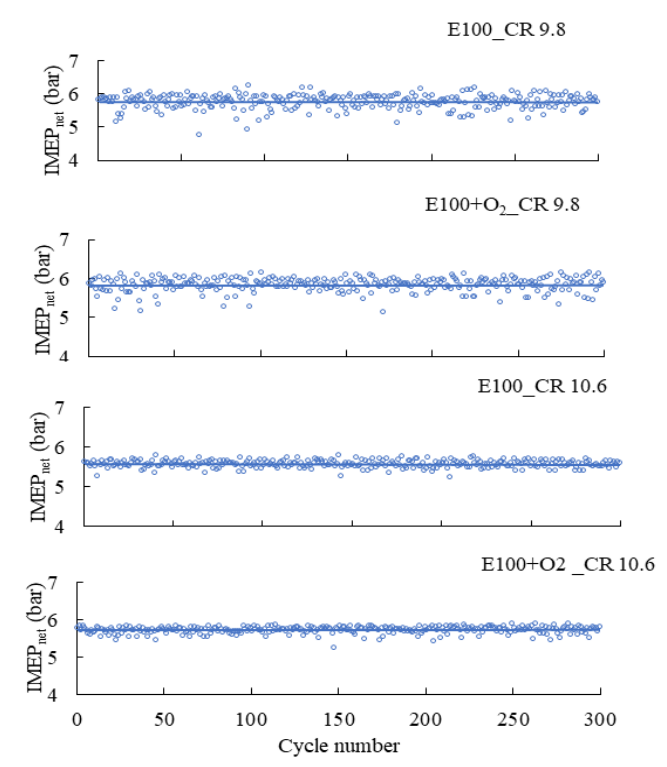


Figure 14. Cycle-to-cycle variations in IMEPnet with E100 at various conditions.

With the combined effect of high compression ratio and oxygen enrichment, the turbulence is dominant further with the additional factor of a decrease in residual gases. High amounts of residual gases hinder the formation of the flame kernel and thus flame development and propagation become difficult. Due to improved combustion, the COV_{IMEP} decreased to 1.48% with M100 and E100. With oxygen enrichment, the mixture formation of air and fuel is improved. The in-cylinder temperature increases and combustion become better. The quality of heat increases which enhances the work output. The flame speed increases and the combustion is completed in less time. All these factors contribute to a decrease in cyclic variations in IMEP. With oxygen enrichment at high compression ratio, the effect is cumulative and cyclic variations decreased further.

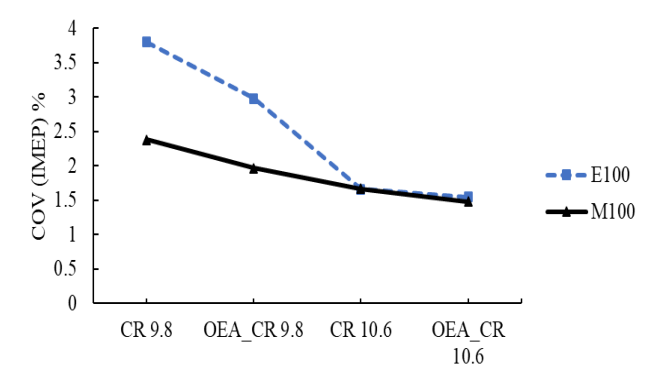


Figure 15. COV_{IMEP} net with M100 and E100 at various conditions.

It is also observed from the figure that at the base condition the COV was less with M100 than with E100. It is due to better combustion with M100 on account of its high laminar flame speed, more oxygen content, and lean burning ability. The high flame diffusivity helps in the formation of a homogenous air-fuel mixture and thus promotes better combustion with M100. In addition to this, the formation of OH radicals is also higher with M100 which is helpful in flame propagation.

3.5 Summary of Discussion

The summary of results and discussion section is tabulated in Table 7. All experimental data in Table 2 are reported at a constant torque of 4.5 Nm, which corresponds to the maximum torque achievable with methanol (M100) under the tested conditions. This torque value was selected as a reference point to ensure a fair and consistent comparison of the combustion and performance characteristics of different fuels under identical load conditions. Evaluating the fuels at the same operating torque eliminates variability due to load differences and isolates the effect of fuel properties, allowing for a more accurate assessment of their performance across various combustion parameters.

Symbol indication: "↑↑↑"- drastic increase, "↑↑"- significant increase, "↑"- moderate increase, "--" - comparable to base gasoline, "↓↓↓"- drastic decrease, "↓↓"- significant decrease, "↓"- moderate decrease

Table 7. Summary of discussion with M100 and E100 fuels.

Parameter	M100 (max. torque)	E100 (lower torque)
Peak cylinder pressure	↑↑↑ ↑ ↑↑	↑ ↑
Max. HRR	↑↑↑ ↑ ↑↑↑	1-↑↑ 2 3-↑↑
Max. ROPR	↑↑↑ ↑↑ ↑↑↑	↑↑ ↑ ↑
Combustion duration	↓	‡ ‡ ‡
Ignition delay	↓↓ ↓ ↓↓	 ↓ ↓

4. Conclusions

Experiments were conducted on a single-cylinder fourstroke spark-ignition engine fuelled with methanol and ethanol to study the combustion characteristics using oxygen-enriched air and increased compression ratio. The important points that emerged from the study are given below:

The P_{max} increased drastically by 56.5% with M100 and by 17.6% with E100 compared to the base gasoline. It increased further significantly with oxygen enrichment at increased compression ratio. The increase in peak pressure was higher with M100 due to its high flame speed, more oxygen content and high reactivity than E100.

The maximum heat release rate increased by more than 92.2% with M100 and by 65.4% with E100 due to oxygen enrichment. High rate of heat release caused the fast burning of fuel and shorten the combustion duration and ignition

delay. Combustion duration shortened by 35.8% with M100 and 28.2% with E100.

Due to oxygen enrichment, the combustion improved resulting in high rate of pressure rise with M100 and E100. The maximum rate of pressure rise increased by 2.5 times with M100 and 40.8% with E100 compared to base gasoline at the base compression ratio. The trend was similar at increased compression ratio and with oxygen enrichment at increased CR.

With oxygen enrichment, the combustion parameters including $P_{\text{max}},$ HRR, and ROPR improved resulting in a decreased cycle-to-cycle to variations. The COVIMEP net decreased from 2.38% to 1.97% with M100 and from 3.8% to 2.98% with E100 with oxygen enrichment.

The effect of oxygen enrichment was more prominent with M100 than E100 at both the compression ratios. The effect was greater at higher compression ratio than the base.

In future work, it's important to explore emissions performance under oxygen-enriched conditions to better understand environmental impacts alongside efficiency gains. Investigating knock tendency, combustion stability over extended cycles, and using advanced diagnostics like optical imaging can offer deeper insights into flame behaviour and in-cylinder dynamics. Studying fuel blends and applying CFD and chemical kinetics modelling could further support optimization. Finally, long-term durability testing is recommended to evaluate the practical feasibility of using oxygen-enriched air with alcohol fuels in real engine applications.

Acknowledgement

Author is thankful to *the Engine and Unconventional Fuels Laboratory, IIT Delhi* where experimental work was carried out during doctoral work under the supervision of Prof. Dr. K. A. Subramanian.

Conflict of Interest

The author approves that to the best of knowledge; there is not any conflict of interest or common interest with an institution/organization or a person that may affect the review process of the paper.

Credit Author Statement

Nidhi: Data Analysis and Interpretation, Writing

Nomenclature

SI	Spark Ignition
CR	Compression Ratio
IC	Internal Combustion
M100	Methanol (100%)
E100	Ethanol (100%)
MX	Methanol blend with X% of gasoline
EX	Ethanol blend with X% of gasoline
BMEP	Brake Mean Effective Pressure
<i>BSFC</i>	Brake Specific Fuel Consumption
IMEP	Indicated Mean Effective Pressure
COV	Coefficient of Variance
BTE	Brake Thermal Efficiency
PV curve	Pressure Volume Curve
VE	Volumetric Efficiency
CO	Carbonmonoxide
HC	Hydrocarbon
NOx	Nitrogen oxides
P_{max}	Peak pressure [bar]

ROPR Rate of Pressure Rise
HRR Heat Release Rate [J/deg.]
(a/b) TDC After/Before Top Dead Centre

OEA Oxygen Enriched Air
OE Oxygen Enrichment
CD Combustion Duration

BS Bharat Stage C.A Crank Angle

 $V_{crevice}$ Crevice volume of cylinder [m³] V_{swept} Swept volume of cylinder [m³] $V_{clearance}$ Clearance volume of cylinder [m³] $V_{clearance\ gap}$ Volume of clearance gap [m³]

B Cylinder bore [mm]
L Cylinder length [mm]
P In-cylinder pressure [bar]
V Instantaneous volume [m³]
γ Ratio of specific heats

Orank angle

References:

- [1] E. Lindstad, T. Ø. Ask, P. Cariou, G. S. Eskeland and A. Rialland, "Wide use of renewable energy in transport," *Transportation Research Part D: Transport and Environment*, vol. 119, June 2023, Art. no. 103713, doi: 10.1016/j.trd.2023.103713.
- [2] S. Shafiee and E. Topal, "When will fossil fuel reserves be diminished?," *Energy Policy*, vol. 37, no. 1, pp. 181–189, Jan. 2009, doi: 10.1016/j.enpol.2008.08.016.
- [3] Z. Tian, X. Zhen, Y. Wang, D. Liu, and X. Li, "Comparative study on combustion and emission characteristics of methanol, ethanol and butanol fuel in TISI engine," *Fuel*, vol. 259, Jan. 2020, Art. no. 116199, doi: 10.1016/j.fuel.2019.116199.
- [4] A. M. Pourkhesalian, A. H. Shamekhi, and F. Salimi, "Alternative fuel and gasoline in an SI engine: A comparative study of performance and emissions characteristics," *Fuel*, vol. 89, no. 5, pp. 1056–1063, May 2010, doi: 10.1016/j.fuel.2009.11.025.
- [5] Y. Li, X.-S. Bai, M. Tunér, H. G. Im, and B. Johansson, "Investigation on a high-stratified direct injection spark ignition (DISI) engine fueled with methanol under a high compression ratio," *Applied Thermal Engineering*, vol. 148, pp. 352–362, Feb. 2019, doi: 10.1016/j.applthermaleng.2018.11.065.
- [6] X. Li, X. Zhen, Y. Wang, and Z. Tian, "Numerical comparative study on performance and emissions characteristics fueled with methanol, ethanol and methane in high compression spark ignition engine," *Energy*, vol. 254, Sept. 2022, Art. no. 124374, doi: 10.1016/j.energy.2022.124374.
- [7] X. Li, X. Zhen, S. Xu, Y. Wang, D. Liu, and Z. Tian, "Numerical comparative study on knocking combustion of high compression ratio spark ignition engine fueled with methanol, ethanol and methane based on detailed chemical kinetics," *Fuel*, vol. 306, Dec. 2021, Art. no. 121615, doi: 10.1016/j.fuel.2021.121615.
- [8] Q. Duan, X. Yin, X. Wang, H. Kou, and K. Zeng, "Experimental study of knock combustion and direct injection on knock suppression in a high compression

- ratio methanol engine," *Fuel*, vol. 311, Mar. 2022, Art. no. 122505, doi: 10.1016/j.fuel.2021.122505.
- [9] T. G. Leone et al., "The Effect of Compression Ratio, Fuel Octane Rating, and Ethanol Content on Spark-Ignition Engine Efficiency," Environ. Sci. Technol., vol. 49, no. 18, pp. 10778–10789, Sept. 2015, doi: 10.1021/acs.est.5b01420.
- [10] O. I. Awad, R. Mamat, M. M. Noor, T. K. Ibrahim, I. M. Yusri, and A. F. Yusop, "The impacts of compression ratio on the performance and emissions of ice powered by oxygenated fuels: A review," *Journal of the Energy Institute*, vol. 91, no. 1, pp. 19–32, Feb. 2018, doi: 10.1016/j.joei.2016.09.003.
- [11] P. Sakthivel, K. A. Subramanian, and R. Mathai, "Effects of different compression ratios and spark timings on performance and emissions of a two-wheeler with 30% ethanol-gasoline blend (E30)," *Fuel*, vol. 277, May 2020, Art. no. 118113 doi: 10.1016/j.fuel.2020.118113.
- [12] M. K. Balki and C. Sayin, "The effect of compression ratio on the performance, emissions and combustion of an SI (spark ignition) engine fueled with pure ethanol, methanol and unleaded gasoline," *Energy*, vol. 71, pp. 194–201, July 2014, doi: 10.1016/j.energy.2014.04.074.
- [13] B. S. Nuthan Prasad, J. K. Pandey, and G. N. Kumar, "Impact of changing compression ratio on engine characteristics of an SI engine fueled with equi-volume blend of methanol and gasoline," *Energy*, vol. 191, Jan. 2020, Art. no. 116605, doi: 10.1016/j.energy.2019.116605.
- [14] C. Wouters, P. Burkardt, and S. Pischinger, "Limits of compression ratio in spark-ignition combustion with methanol," *International Journal of Engine Research*, vol. 23, no. 5, pp. 793–803, May 2022, doi: 10.1177/14680874211043390.
- [15] C. Gong, F. Liu, J. Sun, and K. Wang, "Effect of compression ratio on performance and emissions of a stratified-charge DISI (direct injection spark ignition) methanol engine," *Energy*, vol. 96, pp. 166–175, Feb. 2016, doi: 10.1016/j.energy.2015.12.062.
- [16] M. B. Çelik, B. Özdalyan, and F. Alkan, "The use of pure methanol as fuel at high compression ratio in a single cylinder gasoline engine," *Fuel*, vol. 90, no. 4, pp. 1591–1598, Apr. 2011, doi: 10.1016/j.fuel.2010.10.035.
- [17] Y. Zhou *et al.*, "Potential of compression ratio and exhaust gas dilution on improving combustion and nitrogen oxides emission performance on a PFI engine fueled with methanol," *Fuel*, vol. 323, Sept. 2022, Art. no. 124197, doi: 10.1016/j.fuel.2022.124197.
- [18] L. Li, D. Qiu, and Z. Liu, "The Characteristic of Transient HC Emissions of the First Firing Cycle During Cold Start on an LPG SI Engine," Toronto, Canada, Oct. 2006, doi: 10.4271/2006-01-3403.
- [19] J. A. Caton, "The Effects of Oxygen Enrichment of Combustion Air for Spark-Ignition Engines Using a Thermodynamic Cycle Simulation," in ASME 2005 Internal Combustion Engine Division Spring Technical

- *Conference*, Chicago, Illinois, USA: ASMEDC, pp. 135–147, Jan. 2005, doi: 10.1115/ICES2005-1006.
- [20] P. Seers, F. Foucher, and C. Mounaïm-Rousselle, "Influence of O₂ -enriched intake air with CO₂ dilution on the combustion process of an optically accessible spark-ignition engine," *International Journal of Engine Research*, vol. 14, no. 1, pp. 34–44, Feb. 2013, doi: 10.1177/1468087412442122.
- [21] Nidhi and K. A. Subramanian, "Experimental investigation on effects of oxygen enriched air on performance, combustion and emission characteristics of a methanol fuelled spark ignition engine," *Applied Thermal Engineering*, vol. 147, pp. 501–508, Jan. 2019, doi: 10.1016/j.applthermaleng.2018.10.066.
- [22] J. Jeevahan, A. Poovannan, V. Sriram, R. B. Durai Raj, G. Maghwaran, and G. Britto Joseph, "Effect of intake air oxygen enrichment for improving engine performance and emissions control in diesel engine," *International Journal of Ambient Energy*, vol. 40, no. 1, pp. 96–100, Jan. 2019, doi: 10.1080/01430750.2017.1372811.
- [23] T. T. Maxwell, V. Setty, J. C. Jones, and R. Narayan, "The Effect of Oxygen Enriched Air on the Performance and Emissions of an Internal Combustion Engines," Philadelphia, Pennsylvania, United States, Oct. 1993, Art. no. 932804. doi: 10.4271/932804.
- [24] A. A. Quader, "Exhaust Emissions and Performance of a Spark Ignition Engine Using Oxygen Enriched Intake Air," *Combustion Science and Technology*, vol. 19, no. 1–2, pp. 81–86, Nov. 1978, doi: 10.1080/00102207808946869.
- [25] S. Kajitani, N. Sawa, T. McComiskey, and K. T. Rhee, "A Spark Ignition Engine Operated by Oxygen Enriched Air," San Francisco, California, United States, Oct. 1992, Art. no. 922174. doi: 10.4271/922174.
- [26] R. B. Poola, H. K. Ng, R. R. Sekar, J. H. Baudino, and C. P. Colucci, "Utilizing Intake-Air Oxygen-Enrichment Technology to Reduce Cold-Phase Emissions," Toronto, Canada, Oct. 1995, Art. no. 952420. doi: 10.4271/952420.
- [27] J. Heywood, *Internal Combustion Engine Fundamentals 2E*, 2nd edition. New York, N.Y: McGraw-Hill Education, 2019.
- [28] S. Verhelst, J. W. Turner, L. Sileghem, and J. Vancoillie, "Methanol as a fuel for internal combustion engines," *Progress in Energy and Combustion Science*, vol. 70, pp. 43–88, Jan. 2019, doi: 10.1016/j.pecs.2018.10.001.
- [29] H. Köten, Y. Karagöz, and Ö. Balcı, "Effect of different levels of ethanol addition on performance, emission, and combustion characteristics of a gasoline engine," *Advances in Mechanical Engineering*, vol. 12, no. 7, July 2020, Art. no. 1687814020943356, doi: 10.1177/1687814020943356.
- [30] X. Li, X. Zhen, Y. Wang, and Z. Tian, "Numerical comparative study on performance and emissions characteristics fueled with methanol, ethanol and methane in high compression spark ignition engine,"

- *Energy*, vol. 254, Sept. 2022, Art. no. 124374, doi: 10.1016/j.energy.2022.124374.
- [31] V. Ya. Basevich, S. M. Kogarko, and G. A. Furman, "The reaction of methanol with atomic oxygen," *Russ Chem Bull*, vol. 24, no. 5, pp. 948–952, May 1975, doi: 10.1007/BF00922939.
- [32] P. Geng, H. Zhang, and S. Yang, "Experimental investigation on the combustion and particulate matter (PM) emissions from a port-fuel injection (PFI) gasoline engine fueled with methanol–ultralow sulfur gasoline blends," *Fuel*, vol. 145, pp. 221–227, Apr. 2015, doi: 10.1016/j.fuel.2014.12.067.
- [33] X. Cai, J. Wang, W. Zhang, Y. Xie, M. Zhang, and Z. Huang, "Effects of oxygen enrichment on laminar burning velocities and Markstein lengths of CH4/O2/N2 flames at elevated pressures," *Fuel*, vol. 184, pp. 466–473, Nov. 2016, doi: 10.1016/j.fuel.2016.07.011.
- [34] S. M. Sarathy, P. Oßwald, N. Hansen, and K. Kohse-Höinghaus, "Alcohol combustion chemistry," *Progress in Energy and Combustion Science*, vol. 44, pp. 40–102, Oct. 2014, doi: 10.1016/j.pecs.2014.04.003.
- [35] X. Zhang, Y. Duan, R. Zhang, H. Wei, and L. Chen, "Optical study of oxygen enrichment on methane combustion characteristics under high compression-ratio conditions," *Fuel*, vol. 328, Nov. 2022, Art. no. 125251, doi: 10.1016/j.fuel.2022.125251.
- [36] D. N. Assanis, R. B. Poola, R. Sekar, and G. R. Cataldi, "Study of Using Oxygen-Enriched Combustion Air for Locomotive Diesel Engines," *Journal of Engineering for Gas Turbines and Power*, vol. 123, no. 1, pp. 157–166, Jan. 2001, doi: 10.1115/1.1290590.
- [37] X. Li *et al.*, "Exploring the effects of compression ratio and initial flame kernel radius on combustion characteristics and fuel economy of a dual-fuel spark ignition engine under oxy-fuel combustion mode," *Fuel*, vol. 385, Apr. 2025, Art. no. 134098, doi: 10.1016/j.fuel.2024.134098.
- [38] J. Skřínský, "Measurement and Calculation of Explosion Pressure for Hydroxyl Substituted Hydrocarbons Mixture," MATEC Web Conf., vol. 168, p. 06006, 2018, doi: 10.1051/matecconf/201816806006.
- [39] Z. H. Huang *et al.*, "Combustion characteristics and heat release analysis of a compression ignition engine operating on a diesel/methanol blend," *Proceedings of the Institution of Mechanical Engineers, Part D: Journal of Automobile Engineering*, vol. 218, no. 9, pp. 1011–1024, Sept. 2004, doi: 10.1243/0954407041856818.
- [40] Z. Chen, J. Deng, H. Zhen, C. Wang, and L. Wang, "Experimental Investigation of Hydrous Ethanol Gasoline on Engine Noise, Cyclic Variations and Combustion Characteristics," *Energies*, vol. 15, no. 5, p. 1760, Feb. 2022, doi: 10.3390/en15051760.
- [41] M. Ghaderi Masouleh, K. Keskinen, O. Kaario, H. Kahila, S. Karimkashi, and V. Vuorinen, "Modeling cycle-to-cycle variations in spark ignited combustion engines by scale-resolving simulations for different

- engine speeds," *Applied Energy*, vol. 250, pp. 801–820, Sept. 2019, doi: 10.1016/j.apenergy.2019.03.198.
- [42] J. Zheng, Z. Huang, J. Wang, B. Wang, D. Ning, and Y. Zhang, "Effect of compression ratio on Cycle-by-
- Cycle variations in a natural gas direct injection engine," Energy & Fuels, vol. 23, no. 11, pp. 5357–5366, Nov. 2009, doi: 10.1021/ef900651p.